ENHANCING TOKAMAK CONTROL GIVEN POWER SUPPLY VOLTAGE SATURATION

J-Y. Favez*, Ph. Mullhaupt, B. Srinivasan, D. Bonvin, Laboratoire d'Automatique
J.B. Lister, Centre de Recherches en Physique des Plasmas
Ecole Polytechnique Fédérale de Lausanne, CH-1015 Lausanne, Switzerland

1 INTRODUCTION

The control of the current, position and shape of an elongated cross-section tokamak plasma is complicated by the instability of the plasma vertical position. Linearised models all share the feature of a single unstable pole, attributable to this vertical instability, and a large number of stable or marginally stable poles, attributable to zero or positive resistance in all other circuit equations. Due to the size and therefore the cost of ITER, there will naturally be smaller margins in the Poloidal Field coil power supplies implying that the feedback will experience actuator saturation during large transients due to a variety of plasma disturbances. Current saturation is relatively benign due to the integrating nature of the tokamak, resulting in a reasonable time horizon for strategically handling this problem. On the other hand, voltage saturation is produced by the feedback controller itself, with no intrinsic delay. This paper presents a feedback controller design approach which explicitly takes saturation of the power supply voltages into account when producing the power supply demand signals. We consider the vertically stabilising part of the controller (fast controller) with one power supply and therefore a single saturated input. The method is based on state feedback and therefore requires a reconstruction or an observation of the states of the system. We discuss the feasibility of extracting this state from the available diagnostic information. This novel approach has been tested on simulations using ITER and JET linearised plasma equilibrium response models.

2 DEVELOPMENT OF THE CONTROL METHOD

Throughout this work, we use linearised tokamak models (CREATE-L for JET [1] and ITER [2]) which describe the tokamak by ODEs in the continuous time state space format given by

$$\dot{x}_p = A_p x_p + B_p u + E_p \dot{w} \tag{1}$$

$$y = C_p x_p + F_p w \tag{2}$$

The state variables x_p explicitly represent the physical active coil currents, the passive structure currents and some plasma variables. The coil voltages are the control vector u. The outputs of the system, the vertical and radial plasma positions, wall-separatrix gaps, plasma current and all the magnetic diagnostics measurements, are given by y. The vector $w = \left[\begin{array}{cc} \Delta\beta & \Delta l_i \end{array} \right]^T$ represents disturbances such as ELMs or sawteeth. The power supply voltage saturation is defined by $u = \text{sat}(v)$.

Traditionally, we talk of the vertical position as being unstable. However, when the position is unstable, the passive currents, coil currents and position also grow exponentially, although all these physical variables cannot be considered to be separately unstable. The eigenvalues of the matrix A_p in (1) determine the dynamical evolution of the physical variables x_p. One of the eigenvalues of A_p is positive, expressing the unstable characteristic of the system. However, A_p is not diagonal and therefore the variables x_p are not the eigenvectors of the system. We transform these equations from the variables x_p to new states x for which the transformed matrix A is diagonal, thereby generating the new dynamic representation

$$\dot{x} = Ax + Bu + E\dot{w} \tag{3}$$

$$y = Cx + Fw \tag{4}$$

where $x_p = Tx$, $A = T^{-1}A_pT$, $B = T^{-1}B_p$, $E = T^{-1}E_p$, $C = C_pT$ and $F = F_p$. One of the new orthogonal states is unstable and this is now the single unstable state. Unfortunately, there is no intuitive combination of the physically meaningful variables x_p which describes the unstable state. Furthermore, we can split system (3) into an anti-stable and a stable subsystem

$$\left[\begin{array}{c} \dot{x}_1 \\ \dot{x}_s \end{array} \right] = \left[\begin{array}{cc} \lambda_1 & 0 \\ 0 & A_s \end{array} \right] \left[\begin{array}{c} x_1 \\ x_s \end{array} \right] x + \left[\begin{array}{c} \lambda_1 \\ b_s \end{array} \right] u + \left[\begin{array}{c} E_1 \\ E_s \end{array} \right] \dot{w} \tag{5}$$

Here x_1 and λ_1 describe the anti-stable subsystem and $x_s = \left[\begin{array}{cccc} x_2 & x_3 & \dots & x_n \end{array} \right]^T$, A_s and b_s describe the stable subsystem.

Provided there are sufficient diagnostic measurements, the states can be estimated using the pseudo-inverse of (4)

$$\left[\begin{array}{c} \hat{x} \\ \hat{w} \end{array} \right] = \left[\begin{array}{cc} C & F \end{array} \right]^{\dagger} y \tag{6}$$

reconstructing the unstable state, the stable states, and the disturbance w. If we neglect F (the direct influence of w on y with respect to the nominal equilibrium) then $\hat{x}$ is simple to generate. However, voltage saturation is most likely during a large disturbance and the influence of F must be considered, which is the object of future work.

We have demonstrated that there exists an adequate algebraic state reconstruction such that $\hat{x} \sim x$ (in what follows

* jean-yves.favez@epfl.ch

we use these interchangeably). We can therefore replace an input-output controller $v = Ky$ by a linear state feedback controller

$$v(x) = fx = f_1x_1 + f_2x_2 + f_3x_3 + \ldots + f_nx_n \quad (7)$$

With this feedback controller the closed-loop system becomes $\dot{x} = Ax + B\text{sat}(fx)$.

Our aim is to take an existing controller – labeled the reference controller – and to enlarge its region of attraction $\mathcal{A}$ (the region in state space from which the closed-loop system asymptotically reaches the origin [3, 4]) to the null controllable region $\mathcal{C}$ (the region in state space where there exists an open-loop input that can steer the system to the origin [3, 4]). In previous work we formally considered a system with a single unstable pole and a single stable pole. We derived the region of attraction of the closed-loop system with saturation of the single input [5].

The null controllable region of (5) defined by $\mathcal{C} = \{x \in \mathbb{R}^n : |x_1| < 1\}$ is only restricted by the unstable state (anti-stable system) while the stable states (stable subsystem) can be controlled for any arbitrary values. By considering the linear controller (7), we can see that $\mathcal{A} = \mathcal{C}$ if and only if $f_2 = f_3 = \ldots = f_n = 0$ and if the linear stability condition $1 + f_1 < 0$ is satisfied. But with this the required performance is in general not achievable. However, for all other linear controllers in which at least one of the parameters $f_2,\ f_3\ \ldots\ f_n$ is nonzero, $\mathcal{A} \subset \mathcal{C}$.

We have been able to enlarge the region of attraction to include the full null controllable region $\mathcal{A} = \mathcal{C}$, without loss of local performance, by introducing a continuous nonlinear function in the controller [6, 7]. Consider the modified controller

$$v(x) = f_1x_1 + k(x)(f_2x_2 + f_3x_3 + \ldots + f_nx_n) \quad (8)$$

with $u = \text{sat}(v(x))$. Assume that f has been chosen to obtain the desired performance of the closed-loop system near the origin for small disturbances. Compared to (7), the new controller differs by the introduction of a smooth nonlinearity $k(x)$ by choosing i) within the null controllable region ($|x_1| < 1$), $k(x) = (1 - x_1^2)$ and ii) outside the null controllable region ($|x_1| \geq 1$), $k(x) = 0$. The idea behind this nonlinear controller is as follows. If $x_1 \approx 0$, then $k(x) \approx 1$ and the controller tends towards the linear state feedback controller $v \approx fx$. In this case, the controller concentrates on local performance. On the other hand, if the unstable state approaches the boundary of the null controllable region $\mathcal{C}$, $x_1 \approx \pm 1$ and $k(x) \approx 0$. This implies that the controller tends towards the linear state feedback $v \approx f_1x_1$, and it focuses on the stabilisation of the unstable state and global stability ($\mathcal{A} = \mathcal{C}$). Moreover, since this controller is a continous one, chattering is avoided.

3 TESTING THE METHOD ON ITER

We first implemented this approach on a closed-loop model of ITER. The state was not estimated, but taken directly from the equations. We compare via simulation the reference controller [8], given by (7), against the new continuous nonlinear controller (8) using phase diagrams. Since we are dealing with a high order system (50 .. 100 states) we cannot show the evolution of all states. Thus, the phase diagrams show the evolution of only two states: the unstable state x_1, and one of the most changing stable states, denoted in the figures by x_s. In what follows, the region of attraction of the reference controller is denoted by $\mathcal{A}_r$ and the region of attraction of the continuous nonlinear controller is denoted by $\mathcal{A}_n$. To disturb the system away from the equilibrium we apply an ELM-like disturbance. The disturbance starts at t_0, reaches its maximum at t_1 and vanishes at t_2. Since it is difficult to know whether the state remains in the region of attraction during the disturbance, we have to wait until the disturbance vanishes at t_2 to determine if the controller was able to stabilise the system.

For the first test we do not disturb the system, but we set non-zero initial conditions. The phase diagram (Figure 1) shows the initial conditions point x_{init}, located inside the null controllable region. Since for the nonlinear controller the initial conditions are located in the region of attraction, the trajectory converges to the origin. For the reference controller the trajectory diverges, thus confirming by simulation that $\mathcal{A}_r \subset \mathcal{C}$.

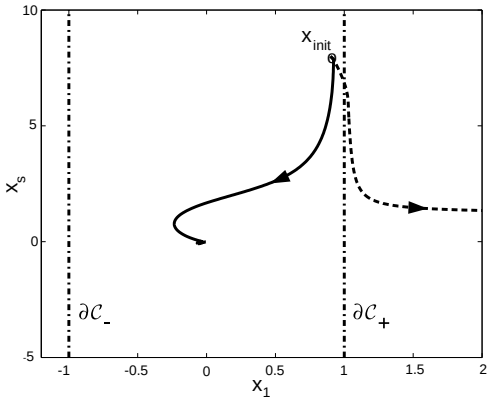

Figure 1: Non-zero initial conditions (x_{init}); dashed: reference controller, solid: continuous nonlinear controller.

The second test shows the evolution of the trajectories for both controllers during and after a large disturbance (Figure 2). At t_2 the states of the closed-loop systems with both controllers are inside $\mathcal{C}$. Since for the nonlinear controller $\mathcal{A}_n = \mathcal{C}$, the trajectory converges to the origin. For the reference controller the trajectory diverges and thus the state is not in $\mathcal{A}_r$.

The third test shows the trajectory for a much larger disturbance amplitude (Figure 3). Both trajectories leave the null controllable region $\mathcal{C}$ and only the trajectory for the system with the nonlinear controller reenters $\mathcal{C}$.

For all these tests, the unstable state x_1 is brought back to the origin faster when the continuous nonlinear controller (8) is used. This is a benefit of the nonlinear function $k(x)$ which helps the controller concentrate on the unstable state in the proximity of the boundaries of $\mathcal{C}$ and beyond it.

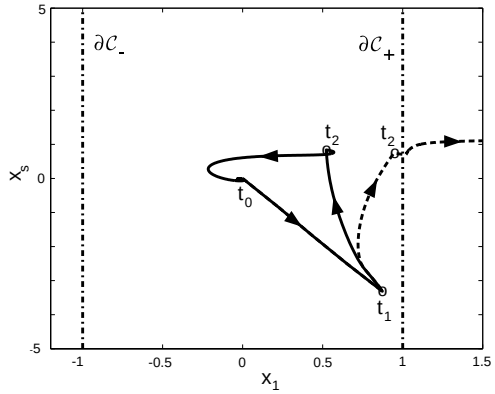

Figure 2: Large disturbance; dashed: reference controller, solid: continuous nonlinear controller.

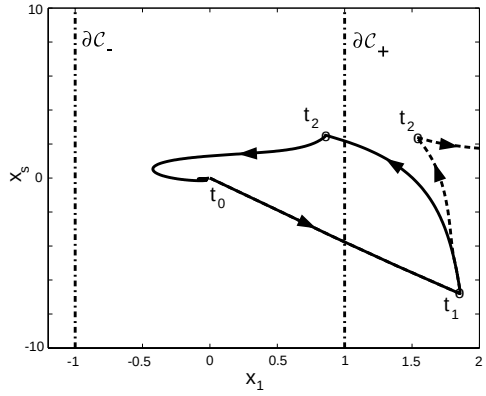

Figure 3: Very large disturbance; dashed: reference controller, solid: continuous nonlinear controller.

4 TESTING THE METHOD ON JET

We implemented this technique on the CREATE-L model of JET, including the closed-loop controller. We generated an estimator of the unstable state directly from the documented diagnostics. We increased the amplitude of the disturbance until the closed-loop model lost control due to saturation of the FRFA (Fast Radial Field Amplifier) supply. The simulation was repeated with the modified controller and control was no longer lost.

Figure 4 shows an example of the evolution of the vertical position z and the FRFA control voltage for a very large ELM disturbance in JET. The disturbance starts at t_0, reaches a maximum at t_1 and vanishes at t_2 (vertical dashed lines). The reference controller loses stability just after t_1.

5 DISCUSSION

A simple continuous nonlinear controller for the stabilisation of the ITER tokamak unstable vertical position in the presence of voltage saturation is proposed. The principle is to modify an existing linear controller by introducing a simple nonlinear term into the control law. This new controller enlarges the region of attraction to the maximal reachable region of attraction under input saturation, which is the null controllable region. Additionally, its local performance around the origin is similar to that of the existing linear controller. An additional advantage of the nonlinear

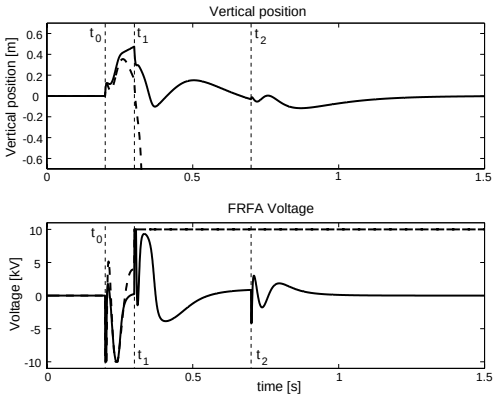

Figure 4: The modifed controller (solid) on a JET simulation. The reference controller (dashed) loses control.

controller is that the unstable state is brought back faster to the origin and thus, the rejection of the disturbance is more efficient. This is a benefit of the nonlinear function where the controller concentrates on the control of the unstable state in the proximity of the boundaries of null controllable region and beyond it.

6 ACKNOWLEDGEMENTS

This work was partly supported by the Fonds National Suisse de la Recherche Scientifique. We thank Y. Gribov, A. Kavin, R. Albanese, F. Villone, G. Calabrò, M. Mattei and A. Pironti for providing the models.

7 REFERENCES

[1] R. Albanese, G. Calabrò, M. Mattei, and F. Villone. Plasma response models for current, shape and position control in JET. In *Proc. SOFT 2002, accepted for publication in Fusion Engineering and Design*, Helsinki, Finland, 2002.

[2] A. Kavin. ITER-FEAT linear models description. In *ITER NAKA JWS, Issue 1*, Naka, Japan, 10 July 2000.

[3] J. Alvarez, R. Suárez, and J. Alvarez. Planar linear systems with single saturated feedback. *System & Control Letters*, 20:319–326, 1993.

[4] T. Hu and Z. Lin. *Control Systems with Actuator Saturation: Analyses and Design*. Birkhauser, Boston, 2000.

[5] J-Y. Favez, B. Srinivasan, Ph. Mullhaupt, and D. Bonvin. Condition for bifurcation of the region of attraction in linear planar systems with saturated linear feedback. In 41^{th} *Conference on Decision and Control*, pages 3918–3923, Las Vegas, USA, 2002.

[6] J-Y. Favez, Ph. Mullhaupt, B. Srinivasan, and D. Bonvin. A globally stabilising controller under saturated input for linear planar systems with one unstable pole. In Submitted to *American Control Conference ACC 2004*, Boston, USA, 2004.

[7] J-Y. Favez, Ph. Mullhaupt, B. Srinivasan, J.B. Lister, and D. Bonvin. Improving the region of attraction of ITER in the presence of actuator saturation. In 42^{th} *Conference on Decision and Control*, Hawaii, USA, 2003.

[8] M. Ariola, A. Pironti, and A. Portone. A reduced-order controller for plasma position and shape control in the ITER-FEAT tokamak. In *CDC00-REG1452, 3 May 2000*.